Author's final submitted manuscript. Published as:
J. Mass Spectrom., vol. 35, pp. 1237-1245 (2000)
DOI: 10.1002/1096-9888(200011)35:11<1237::AID-JMS74>3.0.CO;2-O
URL: http://onlinelibrary.wiley.com/doi/10.1002/1096-9888%28200011%2935:11%3C1237::AID-JMS74%3E3.0.CO;2-O/abstract

On secondary ion-molecule reactions in MALDI

R. Knochenmuss*[1] , A. Stortelder[1], K. Breuker[2], R. Zenobi[1]
1) Laboratory for Organic Chemistry
Swiss Federal Institute of Technology
Universitätsstr. 16
8092 Zürich, Switzerland
2) Dept. of Chemistry and Chemical Biology
Cornell University
Ithaca, NY
14853-1301, USA

*Author for correspondence
tel: ++41 1 632 3875
fax: ++41 1 632 1292
email: knochenmuss@org.chem.ethz.ch

Keywords: MALDI ionization, desorption, proton transfer, electron transfer, ion-molecule reactions

Abstract
Ion-molecule charge and proton transfer reactions in the desorption plume are considered for the case of MALDI with ultraviolet laser excitation, and it is proposed that they are major determinants of the observed mass spectrum. Specific MALDI phenomena which are discussed include: the dominance of singly charged ions, and analyte-matrix or analyte-analyte signal suppression. Should any be formed, highly charged products can be reduced by reaction with neutral matrix, yet singly charged ions cannot generally be neutralized in the same manner. Ion suppression effects can also explained by similar reactions, which in some cases involve interconversion of dissimilar ion types. The plume is proposed to often be more under thermodynamic rather than kinetic control due to these secondary reactions. UV-MALDI mass spectra should therefore be largely predictable, given sufficient thermodynamic information, and appropriate experimental conditions of sufficient analyte and plume density.

Introduction

The well-developed status of matrix-assisted laser desorption/ionization (MALDI) mass spectrometry as an analytical method stands in unsatisfactory contrast to the limited understanding of how it works. In particular, the factors determining the observed ion distribution remain uncertain (1-14). Since MALDI is naturally of greatest interest to mass spectrometrists, the most common approach to testing models of MALDI ionization is to perform MALDI-MS experiments and to vary parameters such as matrix, laser fluence, wavelength, analyte, analyte concentration, etc. Such experiments have led to qualitative mechanistic proposals which include a wide variety of rather different processes (15-17).

This approach is increasingly complemented by non-MALDI experiments which provide information pertaining to individual aspects of MALDI theories(1). These include, for example, ionization potentials and gas-phase acidities and basicities. As relevant physical data become increasingly available, the roles of matrix-matrix, matrix-analyte and analyte-analyte reactions in both primary and secondary ionization events can be more quantitatively evaluated and the wide range of potential mechanisms constrained.

In the case of MALDI with ultraviolet laser excitation (UV-MALDI) we find that thermodynamically limited secondary ion-molecule reactions in the plume are extremely important for understanding the observed mass spectrum. These conclusions are consistent with, and a conceptual extension of numerous earlier indications for ion-molecule reactions. A variety of experiments have suggested that analyte ions are formed either predominantly or in part via secondary reactions with matrix or metal ions, (15, 16, 18-26). Also, there have been suggestions that ion-molecule reaction thermodynamics influence MALDI spectra in a systematic way (9, 16, 23, 26-30). These studies were generally qualitative in nature, but point in the same direction as the model presented here.

We quantitatively consider secondary reaction thermodynamics, and show that important UV-MALDI phenomena, including the matrix and analyte suppression effects, and the dominance of +1 ions can be explained and predicted by these reactions. Knowledge or calculation of quantitative reaction data leads increasingly toward the hypothesis that UV-MALDI mass spectra are largely thermochemically predictable. In the present view, secondary reactions can be so extensive that primary ionization events are not necessarily reflected in the mass spectrum. Primary ionization may be quite complex, and is outside the scope of this article (1). It is also not yet clear to what extent this hypothesis extends to MALDI with infrared excitation, since typical matrices in that case are chemically significantly different.

Methods

The time-of-flight mass spectrometer is a lab-built instrument with a 2 m linear flight tube. A static acceleration field of 21 kV was used. The acquisition was triggered by the 337 nm nitrogen laser pulse (Laser Science Inc., VSL-337NDT, Cambridge, MA, USA) via a photodiode. Ions were detected with a pair of microchannel plates, and the signal acquired on a 1 GS/s LeCroy 9350C (Chestnut Ridge, NY, USA) digital oscilloscope. Each spectrum was passed to a computer for further processing.

Experiments were also performed on a Fourier transform ion cyclotron resonance (FT-ICR) mass spectrometer with a 4.69 Tesla superconducting magnet (Bruker, Fällanden, Switzerland). The RF electronics and Odyssey data acquisition system were from Finnigan (Finnigan FT/MS, Madison, WI, USA). The laboratory-built vacuum system is comprised of a closed cylindrical ion cell of unit aspect ratio and a sample transfer device for insertion of solid material. The instrument operating pressure was below 10^{-8} mbar. The metal target supporting the solid MALDI samples was positioned approximately 15 mm from the cell. A Nd:YAG laser (Continuum, Minilite MLÐ10, Santa Clara, CA, USA) operated at 355 nm was used for desorption/ionization.

Commercially available reagents were used as received. Valinomycin and substance P (Fluka, Buchs, Switzerland) were prepared as methanol solutions. Gramicidin S and substance P were prepared in 1:1 methanol/water, and desalted by drop dialysis using Millipore VS membranes floated on a 0.015 M diammonium citrate solution, adjusted to pH=5 (31). The tripeptide glycyl-glycyl-histidine (Aldrich) was used together with the matrix 2,4,6-trihydroxyacetophenone (Aldrich). Matrix/analyte solutions were prepared by mixing matrix and analyte solutions (0.05 M each, in acetonitrile/water mixture 1:2 by volume) in a glass vial. The solid samples were prepared by successively placing 5 ml drops on the target (about 50 ml total) and allowing to dry until a relatively thick layer of matrix or matrix/analyte crystals completely covered its metal surface.

For study of the fluence dependence of the ion signal, the laser pulse energy on the sample was controlled by varying the time delay between the YAG flashlamp and the QÐswitch triggers. This delay was calibrated against the laser energy using a pyroelectric detector inserted into the beam. The laser spot size on the target was estimated from sample ablation profiles to be about 2×10^{-6} m^2, from which laser fluences were calculated. In the experiments reported in this study, these ranged from 200 J/m^2 to 600 J/m^2. Typical fluences in ultraviolet MALDI are somewhat lower, between 50 J/m^2 and 300 J/m^2 (32). However, the higher fluences were only needed in the experiments with a matrix/analyte concentration of 1:1, but not when pure matrix or lower analyte concentrations were used. Spectra from single laser shots were collected at each fluence.

Ab initio RHF/MP2 quantum chemical calculations were performed with the GAMESS package (33). The internal 6-31G(2d,p) basis set were used, with the recommended (non-Pople) splitting factors for the polarization functions. All geometries were optimized at the 6-31G(2d,p) level before calculation of the MP2 correction. Full counterpoise correction of the basis set superposition error was used for determination of binding energies. This basis set and procedure were found to give reasonably accurate values for the binding energy of $(DHB\text{-}Na)^+$ (1.64 eV vs. 1.58±0.06 eV measured (34)) and the ionization potential of DHB (Koopman approximation: 8.09 eV, vs 8.045 eV measured (35)). They are also similar to those used in other recent related studies (36, 37).

Results and Discussion

Primary matrix ionization in a commonly used UV-MALDI matrix (2,5 dihydroxybenzoic acid, DHB) has been shown to have a time scale for the dominant process of about 2 nanoseconds (38). Given most probable plume velocities of 500-1000 m/s, this corresponds to a forward expansion of 1-2 micrometers. Energy deficit studies suggest that analyte ions may be formed later, at larger distances out to as much as 35 mm, or 35-70 nanoseconds after the laser pulse (3, 19, 24). Similar results were obtained with pulsed extraction TOF experiments (20). Simulations of the plume show that at such times the plume density is still about 10% of the pre-desorption solid (39). Plume temperatures of about 500 K have been also observed (32, 40), so the mean free path of ions and molecules is quite short, only a few molecular diameters, and the collision rate correspondingly high.

These results, along with studies cited in the introduction, clearly support a picture of matrix primary ionization followed by matrix ion-analyte molecule reactions leading to analyte ions. Matrix-matrix reactions are obviously equally possible. Whatever the ion, matrix is the dominant neutral partner in subsequent collisions and secondary reactions, as summarized in Table 1, simply because it is usually present in substantial excess; the ion to neutral ratio in MALDI has been reported as 10^{-4} - 10^{-7} (41, 42). This is not to imply that other reactions cannot or do not take place, such as ion-ion recombination, but they will be less frequent.

*** Table 1 here ***

The secondary electron and proton transfer ion-molecule reactions of Table 1 assume that a variety of ions exist or may exist as a result of primary ionization processes, which are a separate topic of considerable current interest. Positive ions are the focus of most discussion here since this polarity is perhaps more widely used, and the variety of species is larger, as is the number reaction types needed to account for them. This discussion is also restricted to UV-MALDI because typical UV matrices have similar properties which may differ significantly from IR matrices.

In order to understand MALDI, it is natural to seek or induce effects that are unique and thereby give insight. One such characteristic that has been occasionally noted is that UV-MALDI mass spectra are dominated by singly charged ions, even though more highly charged species might be stable (or metastable). Karas, Glückmann, and Schäfer recently examined this in more detail, concluding that it could be important to understanding MALDI ionization mechanisms (17). Those authors also presented a synthesis of ideas about MALDI spanning primary and secondary processes, for which singly charged ions were only one of several indications used.

Another remarkable MALDI phenomenon, and strong indication for the role of matrix-analyte reactions, is the matrix suppression effect (MSE) (43, 44). Analytes of low to medium molecular weight in sufficient concentration can strongly or completely suppress matrix signals in the MALDI mass spectrum. Matrix-analyte reactions evidently proceed to completion if enough analyte is present. There also appears to be a requirement for good mixing of matrix and analyte in the sample prior to desorption, which can be understood as promoting adequate matrix-analyte collisions or interactions, and avoidance of matrix-rich regions.

Both the prevalence of singly charged ions and the MSE are quantitatively examined here, with the finding that secondary in-plume ion-molecule reactions can explain them. In addition we show examples of and explain analyte-analyte suppression effects (ASE), which require similar secondary reactions.

1) Matrix-analyte ion-molecule reactions and the prevalence of singly charged ions in MALDI mass spectra

a) multiply charged ions and free electron capture

One important aspect of a recently proposed mechanism invokes charge-dependent capture rates for free electrons to explain the prevalence of +1 ions in MALDI (17). While we do not rule this out, it should first be explained why the discussion below does not include this process. Some reasons other mechanisms are believed to be much more likely are:

First, significant quantities of free electrons should not long exist, since the electron affinities of molecules similar to typical matrices are more favorable than -1 eV (45), leaving M^- as the primary negative charge carrier.

Second, free electrons (or M^-) are a minority species in the plume, even less abundant than positive ions, by the amount lost to the vacuum (and detectable in the negative polarity mass spectrum). Neutral matrix is more abundant by several orders of magnitude. On statistical grounds ion-neutral reactions should then be more important than electron capture in determining the MALDI spectrum.

In addition there are some open questions about free electron capture rates. While a quadratic dependence of capture rate on ion charge is expected for a point charge model, there can still be large differences in cross section between ions of like charge. For +1 ions these vary by a factor of up to 50 (46). The expected factor of 4 difference between +1 and +2 ions in the electron capture model is small in comparison. For more highly charged ions this has not been extensively studied, but differences have been observed (47).

It should be noted that many other aspects of the recent Karas model are more thermodynamic in nature, rather than kinetic. In these respects the approach of ref. (17) is similar to that presented here, although less quantitative. With these considerations in mind, we next consider how ion-molecule reactions can influence the observed charge states in a MALDI spectrum.

b) Metal adducts and charge transfer

For some analytes a higher charge state than +1 might be anticipated, such as those forming adducts with ions like Ca^{2+} or Cu^{2+}, or peptides that in solution are multiply protonated or deprotonated. Highly charged ions can be (meta)stable in the gas phase, as electrospray shows, but they also have a very substantial internal Coulomb repulsion energy. As a result they can be quite reactive. We consider first multiply charged species with localized rather than distributed charge.

Perhaps the simplest type of matrix-analyte ion-molecule reaction, collisional charge transfer, has been demonstrated for certain combinations of matrix and analyte (26, 48). When the matrix ionization potential (IP) is greater than the IP of the analyte, charge transfer can be efficient:

$$M^+ + A \rightarrow M + A^+$$

Such charge transfer reactions are not widely observed in UV-MALDI since the IPs of matrices are rather low, and usually not greater than those of the analytes (1, 35).

The reverse reaction, charge transfer from neutral matrix to analyte ions has not received much attention, but should be very important in determining the observed MALDI spectrum, by reducing any doubly charged localized ions to the singly charged state, from which further reduction is not possible. As a simple example, consider the fate

of a divalent metal ion, e.g. Cu^{2+}, in the MALDI plume. The gas-phase second IP of Cu is 20.292 eV (49), compared to, for example, a matrix IP of 8.05 eV (2,5 DHB) (35). The reaction:

$$Cu^{2+} + M \rightarrow Cu^{+} + M^{+}$$
$$\Delta G = IP(M) - IP(Cu^{+}) = -12.24 \text{ eV}$$

where M is matrix, is exothermic by about 12 eV. Clearly no divalent copper ions will survive plume collisions. The process will, however, not continue to a fully reduced metal neutral because the first IP of copper is only 7.726 eV. Since this is below that of DHB, the reaction is endothermic. The same picture holds for many other metal ions. The second IPs are all above the first IP of typical matrices, yet the first metal IP is almost always less.

The same is true for divalent ion-neutral analyte complexes. The $(ACu)^{+} \rightarrow (ACu)^{2+} + e^{-}$ reaction energy (second IP of ACu) will be somewhat less than for the free Cu case, but not enough to change the overall picture. The second IP would have to drop below 8 eV, which, due to the Coulomb energy involved, is very unlikely, even taking into account analyte-metal charge transfer. Compare, for example, $(DHB\text{-}Na)^{+} \rightarrow (DHB\text{-}Na)^{2+} + e^{-}$ for which the calculated IP is 11.2 eV, or the IPs of protonated peptides, which are above 10.5 eV (47). Reaction 1 of Table 1 is therefore expected to be very exothermic in essentially all cases.

On the other hand, full reduction of the metal adduct to the neutral, reaction 1, is endothermic because the first IPs of the adducts will be no larger than that of the metal ions, which are (for those metals normally used), below that of the matrix.

The expected products from this type of partial neutralization process have been observed for copper adducts of styrene pentamers (2, 50, 51). The source of copper ions in the sample was a divalent copper salt, but only singly charged ions were observed. High resolution mass spectrometry showed that these adduct ions were indeed reduced to the +1 state, and that no proton loss occured. Similar results have been obtained by other workers using copper and other metals (50, 52).

c) Non-adduct, localized ions and electron transfer

Matrix to analyte electron transfer was presented above in the context of metal ion adducts because the location of the charge and the energetics are known or easily estimated. It is important to note, however, that the same situation will hold for any $A\text{-}R^{2+}$, where R is a local site of multiple ionization (reaction 2). This is because second IPs of typical organic analyte compounds (i.e. the ionization site R) are above 10 eV due to the Coulomb energy, and hence higher than the rather low first IPs of matrices (near 8 eV). At the same time, matrix IPs are below those of many analytes, so analyte ions will not be fully neutralized. If they can be reduced by charge transfer from the matrix, they should only appear in the MALDI spectrum as metal or proton adducts.

These simple energetic considerations are in agreement with the apparent lack of simple dications in MALDI. Most likely they rarely form, since +1 ions are far less energetically costly. In addition, doubly charged polyatomic ions of this type are often at best metastable due to low energy dissociation pathways (53), so the few that might form due to energetic collisions or some other means will rapidly fragment.

d) Metal adducts and proton transfer

A competing and even more common process for partial neutralization of multiply charged ions containing multivalent metal centers is proton loss (reaction 5). The most favorable pathway is expected to be proton transfer to neutral matrix. The thermodynamics of this can be estimated as follows:

$$AMe^{2+} \rightarrow A + Me^{2+} \quad +3.5 \text{ eV}$$
$$A \rightarrow (A\text{-}H)^- + H^+ \quad +14$$
$$M + H^+ \rightarrow MH^+ \quad -8.5$$
$$(A\text{-}H)^- + Me^{2+} \rightarrow ((A\text{-}H)Me)^+ \quad -16$$
$$AMe^{2+} + M \rightarrow ((A\text{-}H)Me)^+ + MH^+ \text{ net= -7 eV}$$

where Me^+ or Me^{2+} are mono and divalent metal ions, A is analyte and M is matrix. The partial reactions are used only to calculate the energetics, and not intended to represent actual reaction steps.

Binding energies of divalent ions with neutrals are not generally available because of charge transfer reactions like those mentioned above for matrix and analyte (54). The estimated binding energy of Mg^{2+} with water is used (82 kcal/mol or 3.56 eV), as extrapolated via high-level calculations from larger, stable clusters (54, 55). For large polar molecules with good (e.g. bidentate) binding sites, the Me^{2+} binding energy could be greater (compare the calculated value for DHB-Mg^{2+}: 6.0 eV), but the overall reaction remains exothermic (net=-4.5 eV). The $(A\text{-}H)^-$ + Me^{2+} binding energy is calculated for $(DHB\text{-}H)^-$ + Mg^{2+}, and the A -> $(A\text{-}H)^-$ + H^+ acidity is typical for carboxylic acids and phenols (45, 56). The matrix basicity is typical of several matrices (14, 29, 57, 58).

This reaction will efficiently reduce +2 complexes to the +1 state, but not neutralize AMe^+, because the first and last partial reactions are about half as energetic:

$$AMe^+ \rightarrow A + Me^+ \quad +1.5 \text{ eV}$$
$$A \rightarrow (A\text{-}H)^- + H^+ \quad +14$$
$$M + H^+ \rightarrow MH^+ \quad -8.5$$
$$(A\text{-}H)^- + Me^+ \rightarrow ((A\text{-}H)Me) \quad -6.2$$
$$AMe^+ + M \rightarrow ((A\text{-}H)Me) + MH^+ \text{ net= +2.9 eV}$$

The Me^+ affinity is typical for sodium with nucleobases (59), and the Me^+ salt binding energy was calculated for an organic acid: $(DHB\text{-}H)^-$ + Na^+.

Products consistent with this mechanism are frequently observed. For example, ions have been observed containing multiple divalent metals (e.g. Ca^{2+}) yet with a net charge of +1, due to proton loss (60). Certain metals seem to favor this pathway, particularly as complex adducts with deprotonated matrix (2, 50, 52, 60). Matrix probably acts as a bidentate ligand in many cases (51).

e) delocalized multiply protonated ions

It is notable that the relatively few doubly or higher charged ions which are observed in MALDI are typically those of relatively large molecules; multiple charging becomes less energetically costly as the charges are more widely distributed. If the charges are very far apart, they will become effectively independent, and not be reduced via the above pathways.

Multiply protonated basic analytes (e.g. proteins) are a particularly important case since they are the most commonly observed +2, +3,... species in MALDI, even though +1 ions still dominate. The incremental proton affinities of a few proteins are known, and lie between 8.5-9 eV for higher charge states; rising to 9.5-10 eV for doubly protonated +2

ions (61, 62). Matrix basicities are 8-9 eV, so proton transfer is favorable or thermoneutral for higher charge states (reaction 6). Even when the reaction is not highly exothermic, the large matrix excess will shift the distribution to low analyte charge states.

$$(AH_n)^{n+} \rightarrow (AH_{n-1})^{(n-1)+} + H^+ \quad 8.5 \text{ to } 10 \text{ eV}$$
$$M + H^+ \rightarrow MH^+ \quad -8 \text{ to } -9$$
$$(AH_n)^{n+} + M \rightarrow (AH_{n-1})^{(n-1)+} + MH^+$$

net <0 eV for larger n, more basic matrix

Clear evidence for such analyte-to-matrix proton transfer reduction has been observed by J¿rgensen, Bojesen and Rahbek-Nielsen (13). Matrices of higher proton affinity yielded lower charge states (essentially only +1) of several proteins, and the effect was more pronounced for smaller proteins which have a larger internal Coulomb energy. This is fully consistent with a proton transfer reduction mechanism.

For all charges states down to +2 another favorable reduction pathway may be charge transfer and reduction of protons (reaction 3):

$$(AH_n)^{n+} + e^- \rightarrow (AH_{n-1})^{(n-1)+} + H \quad -6 \text{ to } ? \text{ eV}$$
$$M \rightarrow M^+ + e^- \quad +8.05$$
$$(AH_n)^{n+} + M \rightarrow M^+ + (AH_{n-1})^{(n-1)+} + H \quad \text{net } <0 \text{ eV?}$$

The energetics of the first half reaction are not known, but estimates have been made to help understand the recently developed electron capture dissociation method (47). An energy release of 5-7 eV was proposed as a rough estimate, and is determined to a great extent by the Coulomb well into which the electron falls. Even for protons distributed 17 Ångstroms apart on an analyte, an incoming electron releases 1 eV per extra proton charge (63). A doubly protonated molecule might have an electron affinity (top partial reaction) in the range of 8 eV, if the intrinsic IP of the protonated site is about 6 eV, and the second proton is 9 Å away (2 eV proton-proton Coulomb energy). For comparison, this is the distance between the protonation sites of doubly protonated gramicidin S (64). More highly charged ions will have affinities higher by steps of about 2 eV per proton. This would enable reduction by charge transfer from the matrix. Reduction of +1 ions, on the other hand, will always be impossible, since only the 6 eV intrinsic IP energy is available. In possible support of this mechanism it may be noted that neutral H atoms have been observed in the MALDI plume (65).

The energetics for the charge transfer mechanism do not change as dramatically with increasing charge as for the others above, which would explain the modest amounts of multiply protonated peptides that are often observed in MALDI. The reaction may therefore also be sensitive to minor changes in matrix IP, so the small increments available from matrix dimers or larger clusters may be important for reduction in early phases of the plume expansion (66).

2) Matrix-analyte or analyte-analyte suppression effects and ion interconversion reactions

If secondary ion-molecule reactions are able to explain the charge state distribution in UV-MALDI, it is natural to ask if they can explain relative ion intensities as well. This would be particularly valuable for understanding if or when UV-MALDI can be used in a quantitative manner.

A dramatic effect involving signal intensities in MALDI is the matrix suppression effect (MSE). We next show that the MSE can also be understood as a consequence of secondary ion-molecule reactions and their thermodynamics. Analagous analyte-analyte suppression effects can be predicted from the same model, and are shown to exist, both for similar (protonated) and dissimilar (protonated vs. sodiated) analyte ions.

a) proton transfer reactions and the matrix suppression effect

Analytes such as peptides and proteins have rather high proton affinities (61, 62, 64, 67), larger than that of typical matrices (14, 29, 57, 58). It is therefore easy to imagine that plume proton transfer reactions could lead to depletion of protonated matrix, MH^+, by analyte. This reaction could completely suppress MH^+ if enough analyte were present, and sufficiently well distributed in the sample to come into contact with MH^+ in the plume. Clear indication of such matrix-analyte proton transfer reactions was recently found in the correlation of analyte internal energy with the energy of proton transfer to the matrix (30).

One example of matrix suppression based on proton transfer reactions is that of the tripeptide glycyl-glycyl-histidine (GGH) in the matrix 2,4,6 trihydroxyacetophenone (THAP). In positive mode, the dominant matrix and analyte ions are protonated. Some sodium adducts are observed if the sample is not thoroughly desalted. As is typical for the matrix suppression effect (43, 44), and as will be reported in more detail elsewhere, addition of sufficient GGH to THAP leads to complete loss of matrix signal, while protonated analyte signal remains strong.

The proton affinity of THAP has been determined to be 9.14 eV. (68) Because typical entropy contributions at 300 K are near 0.3 eV (69), the gas-phase basicity of THAP, GB(THAP) should be close to 8.8 eV. The gas-phase basicity of deprotonated THAP, GB((THAP - H)$^-$), was found to be 13.72 eV (57). The GB of glycyl-glycyl-histidine is 10.15 eV (69).

With this information in hand, it may first be noted that potential proton transfer reactions for generating primary ions are remarkably low in energy:

$$THAP + THAP \rightarrow (THAP+H)^+ + (THAP-H)^- \quad DG = +4.9 \text{ eV}$$
$$THAP + GGH \rightarrow (THAP-H)^- + (GGH+H)^+ \quad +3.6$$
$$THAP + GGH \rightarrow (THAP+H)^+ + (GGH-H)^- \quad +5.2$$

Some of the protonated GGH signal may therefore be generated in a primary step, and not in a secondary reaction. Matrix suppression requires that added analyte have a strong effect on matrix ion signal. The ion-molecule reaction required for positive mode suppression in this system is that of protonated matrix with neutral analyte, and is found to be significantly exoergic:

$$(THAP+H)^+ + GGH \rightarrow THAP + (GGH+H)^+ \quad DG = -1.3 \text{ eV}$$

The observed MSE results are thus in accord with the gas phase thermodynamics of the species involved. Clearly, however, matrix suppression requires that any protonated matrix formed be able react with neutral analyte. This is the reason that a rather high analyte concentration is needed for suppression (43). In addition, there must be sufficient plume collisions for the reaction to proceed to completion. This can be seen from Fig. 1, showing the intensities of $(THAP+H)^+$ and $(GGH+H)^+$ as a function of laser fluence. Matrix suppression is reached only at fluences somewhat above threshold, and continues for all higher fluences.

**** Figure 1 here ****

b) matrix ion interconversion reactions and the matrix suppression effect

The THAP / GGH system can be successfully treated as a set of proton transfer reactions. In general, however, the matrix suppression effect is notable for the disappearance of all matrix ions, regardless of ion type (e.g. M^+, MH^+ or MNa^+), and regardless of analyte ion type (protonated or cationized) (43, 44). Since suppression is not limited to the analyte ion type (e.g. MH^+ suppressed by AH^+, or MNa^+ by ANa^+), a general picture of the MSE must involve more than simple proton competition mechanisms (70, 71). This characteristic of the MSE can be explained by interconversion of matrix ions. These will next be shown to possible via secondary ion-molecule reactions.

In considering these, the range of possible collision energies is important to establish an upper endothermicity limit for the reactions. Although the expanded plume is not very hot, plume collisions in the early phase of the expansion are expected to be quite energetic due to the broad range of stream velocities (72), with estimates of 1.5 eV or more (1, 73). Experimentally, numerous results point to energetic collisions in the plume. Species with known dissociation thresholds as high as 1.3 eV have been found to fragment in MALDI plumes (73), and "in-source decay" or plume fragmentation is an established method for structure elucidation of peptides (74). In addition to the relatively specific fragmentation exploited for in-source decay, MALDI spectra often show a substantially elevated "chemical noise" baseline, with nonspecific fragments at essentially every m/z below that of the analytes (17). It currently seems reasonable to assume that <1 eV collisions are sufficiently numerous that reactions of this endothermicity can be safely considered.

Consider first the interconversion reaction connecting matrix radical cations with protonated matrix (reaction 7):

$$M^+ \rightarrow (M\text{-}H) + H^+ \quad +8.90 \text{ eV}$$
$$M + H^+ \rightarrow MH^+ \quad -8.53$$
$$M^+ + M \rightarrow MH^+ + (M\text{-}H) \quad \text{net} = +0.37 \text{ eV}$$

The values are for 2,5 DHB as measured by bracketing (14). The 2,5 isomer is not unique, this reaction is even more nearly thermoneutral for the other dihydroxybenzoic acid isomers (14).

The reverse of reaction 7 is only slightly exothermic, but neutral M-H is not expected to be abundant, so other reactions may be more important in generating M^+ from MH^+ (reaction 4, the energies are for 2,5 DHB):

$$MH^+ \rightarrow M + H^+ \quad +8.53 \text{ eV}$$
$$M \rightarrow M + e^- \quad +8.05$$
$$H^+ + e^- \rightarrow 1/2(H_2) \quad -15.85$$
$$MH^+ + M \rightarrow M^+ + M + 1/2(H_2) \quad \text{net} = +0.73 \text{ eV}$$

Although the neutral matrix formally cancels out, it is retained to emphasize the necessity for a moderately energetic collision.

Next the proton transfer reaction connecting sodiated and protonated matrix ions (reaction 8, energies for 2,5 DHB):

$$M + M \rightarrow MH^+ + (M\text{-}H)^- +5.25 \text{ eV}$$
$$MNa^+ \rightarrow M + Na^+ +1.58$$
$$(M\text{-}H)^- + Na^+ \rightarrow (M\text{-}H)Na -6.2$$
$$MNa^+ + M \rightarrow MH^+ + (M\text{-}H)Na \text{ net= } -0.3 \text{ eV}$$

The last partial reaction is calculated, the other quantities are known experimentally (34, 57). This is again a low energy reaction. That matrix salts can exchange or donate cations in plume reactions has already been suggested from the beneficial effect of added matrix salts for cationization of polymers (28, 75).

These matrix ion-molecule reactions will lead to facile interconversion of M^+, MH^+ and MNa^+ in the hot plume. As a result, it is clear why all ions are suppressed in the MSE. When a highly favorable matrix-analyte reaction is coupled to one of the reactions in this system (and sufficient encounters occur in the plume) charge will be efficiently drained from all matrix species (reaction 10, Table 1). Another important consequence of these reactions is that the presence (or absence) of matrix radical cations in the mass spectrum is not necessarily an indicator of direct or indirect photoionization in primary ion generation.

c) analyte-analyte suppression and proton transfer

If secondary plume reactions are extensive enough to interconvert the various matrix ion types, leading to the MSE, they presumably can also enable analyte-analyte reactions, and an analyte suppression effect (ASE). This is more complex than matrix suppression, since both direct and matrix-mediated routes need to be considered. The matrix-mediated process will only be active if the respective partial reactions are reversible, or favorable in the direction of suppression. Consider two protonating analytes:

$$AH^+ + M \rightarrow A + MH^+$$
$$B + MH^+ \rightarrow BH^+ + M$$
$$AH^+ + B \rightarrow A + BH^+$$

In this case the order of proton affinities must be PA(A) < PA(M) < PA(B).

Alternatively, if the two analytes are sufficiently concentrated and well mixed in the sample, the probability of analyte-analyte collisions could become high enough for suppression via direct reaction:

$$AH^+ + B \rightarrow A + BH^+$$

Here the only requirement for suppression is that PA(A) < PA(B). An example of analyte suppression which probably follows this picture is shown in Fig. 2. Substance P can fully suppress Gramicidin S (GS) at the appropriate A:B:M concentration ratios. The proton affinity of substance P is not known, but those of the singly protonated ions are: $PA(PH^+)$= 9.82 eV (62), $PA(GSH^+)$= 9.51 eV (64). The order of the PAs for the neutrals will very likely be the same (76, 77). Substance P is therefore expected to deprotonate GSH^+ in a direct reaction. This result is consistent with, and a logical extension of earlier reports that some analytes influence each other in a systematic manner, consistent with their proton affinities (27, 78)

**** Figure 2 here ****

The matrix-mediated process is not favorable, because the PAs of P and GS are both substantially larger than that of the DHB matrix (8.87 eV). That this process proceeds via direct analyte interaction is suggested by the fact that at lower concentration vs matrix

(but the same P:GS ratio), the GS signal reappears. Suppression in this system is also dependent on careful sample preparation to achieve homogenous co-crystallization, as indicated by similar results at various spots on the sample. When this is not the case, differing P/GS signal ratios are observed.

In such a reaction uniform pre-desorption analyte distribution and high post-desorption analyte collision rate are important, so the effect is large only in certain A:B:M concentration ranges, even in this simple case of two protonating analytes. The (A+B):M ratio of Fig 2 is 1:700, which is very similar to the 1:1000 A:M ratios where matrix suppression begins for a variety of analytes (43, 44). In those earler studies it was concluded that this concentration range is where typical in-plume diffusion ranges fall below about 10 matrix diameters, enabling efficient ion-molecule interactions (43).

d) analyte-analyte suppession involving dissimilar ion types

The analyte suppression effect is not limited to simple analyte pairs as above, and reactions involving dissimilar ions are not unique to matrix, as can be seen in Fig. 3.

**** Fig 3 here ****

The quantity of substance P in the sample has a dramatic effect on the signal strength of sodiated valinomycin. A suppression effect is observed, analogous to that for matrix. Instead of appearing as a new signal along with a constant valinomycin peak, P causes the valinomycin signal to vanish.

Substance P appears nearly exclusively as a protonated ion, and valinomycin, being an ionophore, is strongly preferentially cationized with Na^+ ions. There cannot be simple competition between these analytes for protons or cations, they clearly interact with each other via more complex reaction pathways.

Secondary reactions mediated by neutral matrix could enable analyte-analyte interconversions, leading to effects as in Fig 3. Substance P can suppress sodiated valinomycin in the following manner (reaction 9):

$$P + MH^+ \rightarrow PH^+ + M$$
$$M + MNa^+ \rightarrow MH^+ + (M\text{-}H)Na$$
$$ValNa^+ + M \rightarrow MNa^+ + Val$$
$$\_\_\_\_\_$$
$$P + ValNa^+ + M \rightarrow PH^+ + Val + (M\text{-}H)Na$$

By means of such reactions, a particularly stable ion can drain charge out of all the other coupled species, matrix and analytes, provided again that enough of the relevant compound is present and well distributed in the sample. In Fig. 3, this reaction appears to lead to PH^+, which is perhaps to be expected since proton affinities are usually greater than sodium ion affinites, as discussed for specific cases in section 1 above.

The energetics of these reactions are not yet known, so the probabilities of the matrix-mediated and direct reactions cannot be evaluated. The first reaction is certainly exothermic, and the second was shown above to be nearly thermoneutral, so only the relative sodium affinities of Val and M need be determined. As an ionophore, that of Val is probably larger that that of the matrix, but if they differ by less than the collision energy in the plume, the matrix-mediated interconversion should predominate.

e) primary vs. secondary ions and full vs. partial plume equilibrium

The discussion presented above shows that the matrix and analyte suppression effects are consistent with the thermodynamics of secondary plume reactions. This does not rule out important thermodynamic or kinetic factors during primary ionization as well. Indeed,

reactions that are favorable in the plume will probably also be so before large-scale expansion has occured. The present indications are that secondary reactions are more important than earlier realized, but this in no way invalidates any proposals for primary mechanisms.

The reactions discussed above are sufficient to explain a great deal of the known MALDI phenomenology, especially some unusual MALDI effects. They share the common important feature that they are ion-neutral reactions, the neutral usually being matrix, sometimes analyte. If the MALDI plume were to reach full, true equilibrium, no ions (except the net positive charge due to electron loss) would remain at all due to cation-anion neutralization reactions. Ions are minority species and ion-ion encounters evidently remain sufficiently infrequent that full equilibrium is not attained. This is obviously a requirement if MALDI is to give useful results. Ion-neutral matrix collisions are, on the other hand, several orders of magnitude more common because of the abundance of matrix (or neutral analyte), and such reactions do reach or approach a thermodynamically limited ion distribution. In limited concentration ranges, analyte-analyte ion-molecule reactions evidently also become significant and can lead to significant effects in the spectra.

Conclusions

The observed UV-MALDI ions give clear indications of extensive secondary in-plume ion-molecule reactions. Charge and proton transfer reactions, both involving neutral matrix in collisions, are shown both generally and by specific quantitative examples to explain both the singly charged nature of the dominant MALDI ions and the MSE and ASE effects.

The thermodynamics of ion-molecule reactions are such that more highly charged ions are readily reduced in charge state, yet monovalent ions cannot be neutralized in the same manner. Given sufficient plume collisions, the MALDI spectrum may therefore be dominated by singly charged ions (or those with separated multiple monovalent sites).

Suppression effects suggest efficient interconversion of various matrix ion types. For 2,5 DHB these reactions can be quantitatively treated, and are found to be nearly thermoneutral, as expected. The observation of any particular ion therefore gives by itself only indirect information about primary ionization processes.

Matrix-mediated interconversions between dissimilar analyte ions also appear to be active, as for (substance P)H^+ and valinomycin-Na^+ ions. Direct analyte-analyte ion-molecule reactions may be important under certain conditions, as probably observed for substance-P with Gramicidin S.

These results provide quantitative evidence supporting the hypothesis that secondary ion-molecule reactions in the UV-MALDI plume are frequently more under thermodynamic rather than kinetic control. To the extent that the relevant thermochemical values are known, and the experimental conditions are correctly selected, it should be possible to rationally plan and predict many UV-MALDI experiments. The main conditions for this appear to be adequate mixing of matrix and analytes in the sample, and sufficient laser fluence to generate a collision-rich plume.

Possible applications and tests of this model may include better understanding and control of analyte-analyte interferences in mixtures such as protein digests, and improved strategies for quantitative UV-MALDI. It remains to be seen if the same concepts are equally applicable in IR-MALDI.

Acknowledgments

This work as supported by ETH internal research grant 0-20-402-97.

Literature Cited

1. Zenobi R., Knochenmuss R. *Mass Spectrom. Rev.* 1998; **17:** 337.
2. Knochenmuss R., Lehmann E., Zenobi R. *Eur. Mass Spectrom.* 1998; **4:** 421.
3. Kinsel G. R., Gimon-Kinsel M. E., Gillig K. J., Russell D. H. *J. Mass Spectrom.* 1999; **34:** 684.
4. Land C. M., Kinsel G. R. *J. Am. Soc. Mass. Spectrom.* 1998; **9:** 1060.
5. Dreisewerd K., Schurenberg M., Karas M., Hillenkamp F. *Int. J. Mass Spectrom. Ion Proc.* 1996; **154:** 171.
6. Ens W., Schürenberg M., Hillenkamp F., in *45th ASMS Conference on Mass Spectrometry and Allied Topics*, Palm Springs, CA, 1997, 1099.
7. Hoberg A.-M., Haddleton D. M., Derrick P. M. *Eur. Mass Spectrom.* 1997; **3:** 471.
8. Donovan McCarley T., McCarley R. L., Limbach P. A., in *46th ASMS Conf. Mass Spectrom. Allied Top.*, Orlando, FL,1998.
9. Olumee Z., Vertes A. *J. Phys. Chem. B* 1998; **102:** 6118.
10. Tang X., Sadeghi M., Olumee Z., Vertes A. *Rapid Commun. Mass Spectrom.* 1997; **11:** 484.
11. Allwood D. A., Dyer P. E., Dreyfus R. W. *Rapid Commun. Mass Spectrom.* 1997; **11:** 499.
12. Bökelmann V., Spengler B., Kaufmann R. *Eur. Mass Spectrom.* 1995; **1:** 81.
13. Jørgensen T. J. D., Bojesen G., Rahbek-Nielsen H. *Eur. Mass Spectrom.* 1998; **4:** 39.

14. Mormann M., Bashir S. M., Derrick P. J., Kuck D. *J. Am. Soc. Mass Spectrom.* 2000; **11:** 544.
15. Ehring H., Karas M., Hillenkamp F. *Org. Mass Spectrom.* 1992; **27:** 427.
16. Liao P.-C., Allison J. *J. Mass Spectrom.* 1995; **30:** 408.
17. Karas M., Glückmann M., Schäfer J. *J. Mass Spectrom.* 2000; **35:** 1.
18. Spengler B., Kaufmann R. *Analusis* 1992; **20:** 91.
19. Zhou J., Ens W., Standing K. G., Verentchikov A. *Rapid Commun. Mass Spectrom.* 1992; **6:** 671.
20. Wang B. H., Dreisewerd K., Bahr U., Karas M., Hillenkamp F. *J. Am. Soc. Mass Spectrom.* 1993; **4:** 393.
21. Mowat I. A., Donovan R. J. *Rapid Comm. Mass Spectrom.* 1995; **9:** 82.
22. Ehring H., Costa C., Demirev P. A., Sundqvist B. U. R. *Rapid Commun. Mass Spectrom.* 1996; **10:** 821.
23. *Steps Toward a More Refined Picture of the Matrix Function in UV MALDI*, Large Ions: Their Vaporization, Detection and Structural Analysis, T. Baer, C. Y. Ng and I. Powis, Eds.; Wiley and Sons Ltd: London, 1996; 27.
24. Kinsel G. R., Edmondson R. D., Russell D. H. *J. Mass Spectrom.* 1997; **32:** 714.
25. Niu S., Zhang W., Chait B. T. *J. Am. Soc. Mass Spectrom.* 1998; **9:** 1.
26. Macha S. F., McCarley T. D., Limbach P. A. *Anal. Chim. Acta* 1999; **397:** 235.
27. Philips D. R., Karas M., Ehring H., Hillenkamp F. *Proceedings of the 40th Conference on Mass Spectrometry and Allied Topics.* 1993; **:** 372.
28. King R. C., Owens K. G., in *43rd ASMS Conference on Mass Spectrometry and Allied Topics*, Atlanta, GA, 1995, 1238.
29. Burton R. D., Watson C. H., Eyler J. R., Lang G. L., Powell D. H., Avery M. Y. *Rapid Commun. Mass Spectrom.* 1997; **11:** 443.
30. Stevenson E., Breuker K., Zenobi R. *J. Mass Spectrom.* 2000; **35:** 1035.
31. Maruzyk R., Sergeant A. *Anal. Biochem.* 1980; **105:** 403.
32. Dreisewerd K., Schurenberg M., Karas M., Hillenkamp F. *Int. J. Mass Spectrom. Ion Proc.* 1995; **141:** 127.
33. Schmidt M. W., Baldridge K. K., Boatz J. A., Elbert S. T., Gordon M. S., Jensen J. J., Koseki S., Matsunaga N., Nguyen K. A., Su S., Windus T. L., Dupuis M., Montgomery J. A. *J. Comput. Chem.* 1993; **14:** 1347.
34. Zhang J., Stevenson E., Zenobi R. in preparation.
35. Karbach V., Knochenmuss R. *Rapid Commun. Mass Spectrom.* 1998; **12:** 968.
36. Hoyau S., Ohanessian G. *Chem. Eur. J.* 1998; **8:** 1561.
37. Herreros M., Gal J.-F., Maria P.-C., Decouzon M. *Eur. Mass Spectrom.* 1999; **5:** 259.
38. Knochenmuss R., Vertes A. *J. Phys. Chem. B* 2000; **104:** 5406.
39. Vertes A., Irinyi G., Gijbels R. *Anal. Chem.* 1993; **65:** 2389.
40. Mowry C. D., Johnston M. V. *J. Phys. Chem.* 1994; **98:** 1904.
41. Mowry C., Johnston M. *Rapid Comm. Mass Spectrom.* 1993; **7:** 569.
42. Quist A. P., Huth-Fehre T., Sunqvist B. U. R. *Rapid Commun. Mass Spectrom.* 1994; **8:** 149.
43. Knochenmuss R., Karbach V., Wiesli U., Breuker K., Zenobi R. *Rapid Commun. Mass Spectrom.* 1998; **12:** 529.
44. Knochenmuss R., Dubois F., Dale M. J., Zenobi R. *Rapid Commun. Mass Spectrom.* 1996; **10:** 871.
45. Harrison A. G. *Chemical Ionization Mass Spectrometry*, 2nd ed.; CRC Press: Boca Raton, 1992.
46. Franklin J. L. *Ion Molecule Reactions*; Butterworths: London, 1972; Vol. 2.
47. Zubarev R., Horn D. M., Fridriksson E. K., Kelleher N. L., Kruger N. A., Lewis M. A., Carpenter B. K., McLafferty F. W. *Anal. Chem.* 2000; **72:** 563.
48. McCarley T. D., McCarley R. L., Limbach P. A. *Anal. Chem.* 1998; **70:** 4376.
49. *Handbook of Chemistry and Physics*, Lide D. R., Ed. CRC Press: Boca Raton, 1992.
50. Rashidezadeh H., Guo B. *J. Am. Soc. Mass Spectrom.* 1998; **9:** 724.
51. Lehmann E., Knochenmuss R., Zenobi R. *Rapid Commun. Mass Spectrom.* 1997; **11:** 1483.
52. Wong C. K. L., Chan T. W. D. *Rapid Commun. Mass Spectrom.* 1997; **11:** 513.
53. Schröder D., Schwarz H. *J. Phys. Chem.* 1999; **103:** 7385.

54. Peschke M., Blades A. T., Kebarle P. *J. Phys. Chem. A* 1998; **102:** 9978.
55. Pavlov M., Siegbahn P. E. M., Sandstršm M. *J. Phys. Chem. A* 1998; **102:** 219.
56. Jouvet C., Lardeux-Dedonder C., Richard-Viard M., Solgadi D., Tramer A. *J. Phys. Chem.* 1990; **94:** 5041.
57. Breuker K., Knochenmuss R., Zenobi R. *Int. J. Mass Spectrom.* 1999; **184:** 25.
58. Steenvoorden R. J. J. M., Breuker K., Zenobi R. *Eur. Mass Spectrom.* 1997; **3:** 339.
59. Cerda B. A., Wesdemiotis C. *J. Am. Chem. Soc.* 1996; **118:** 11884.
60. Dubois F., Knochenmuss R., Steenvoorden R. J. J. M., Breuker K., Zenobi R. *Eur. Mass Spectrom.* 1996; **2/3:** 167.
61. Zhang X., Cassady C. J. *J. Am. Soc. Mass Spectrom.* 1996; **7:** 1211.
62. Carr S. R., Cassady C. J. *J. Mass Spectrom.* 1997; **32:** 959.
63. Gronert S. *J. Mass Spectrom.* 1999; **34:** 787.
64. Gross D. S., Williams E. R. *J. Amer. Chem. Soc.* 1996; **118:** 202.
65. Scott C. T. J., Kosmidis C., Jia W. J., Ledingham K. W. D., Singhal R. P. *Rapid Commun. Mass Spectrom.* 1994; **8:** 829.
66. Knochenmuss R., Karbach V., Lin Q., in *47th ASMS Conference on Mass Spectrometry and Allied Topics*, Dallas, TX, 1999, 1059.
67. Carr S. R., Cassidy C. J. *J. Am. Soc. Mass Spectrom.* 1996; **7:** 1203.
68. Nelson C. M., Zhu L., Tang W., Smith L. M., Crellin K., Berry J., Beauchamp J. L. *SPIE* 1996; **2680:** 247.
69. *Proton Affinity Evaluation*, NIST Chemistry Webbook, NIST Standard Reference Database No. 69, W. G. Mallard and P. J. Linstrom, Eds.; National Institute of Standards and Technology: Gaithersburg, MD 20899 (http://webbook.nist.gov), 1998.
70. Chan T.-W. D., Colburn A. W., Derrick P. J. *Org. Mass Spectrom.* 1991; **26:** 342.
71. Chan T.-W. D., Colburn A. W., Derrick P. J. *Org. Mass Spectrom.* 1992; **27:** 53.
72. Zhigilei L. V., Garrison B. J. *Rapid Comm. Mass Spectrom.* 1998; **12:** 1273.
73. Breuker K. *Proton Transfer Reactions in Matrix-assisted Laser Desorption Ionization*. Doctoral Thesis, Eidgenšssische Technische Hochschule, ZŸrich, 1999.
74. Reiber D. C., Brown R. S., Weinberger S., Kenny J., Bailey J. *Anal. Chem.* 1998; **70:** 1214.
75. King R. C., Goldschmidt R., Xiong Y., Owens K. G., in *43rd ASMS Conference on Mass Spectrometry and Allied Topics*, Atlanta, GA, 1995, 1237.
76. Wu J., Lebrilla C. B. *J. Amer. Soc. Mass Spectrom.* 1995; **6:** 91.
77. Williams E. R. *J. Mass Spectrom.* 1996; **31:** 831.
78. Zhu Y. F., Lee K. L., Tang K., Allman S. L., Taranencko N. I., Chen C. H. *Rapid Commun. Mass Spectrom.* 1995; **9:** 1315.

Table 1. Summary of potentially important MALDI ion-molecule plume reactions. A, B=analytes, $(A-H)^-$= deprotonated analyte, M= matrix, $(M-H)^-$= deprotonated matrix, Me=metal ion, R=localized analyte ionization site

Electron Transfer

1) metal adduct partial reduction:

$$AMe^{2+} + M \rightarrow AMe^{+} + M^{+}$$

2) localized partial reduction:

$$A\text{-}R^{2+} + M \rightarrow A\text{-}R^{+} + M^{+}$$

3) reduction of protons on multiply protontated analyte:

$$(AH_n)^{n+} + (n-1)M \rightarrow AH^{+} + (n-1)M^{+} + (n-1)H$$

4) matrix protonated → radical cation conversion:

$$MH^{+} + M \rightarrow M^{+} + M + 1/2(H_2)$$

Proton Transfer

5) metal adduct net charge state reduction:

$$AMe^{2+} + M \rightarrow ((A-H)Me)^{+} + MH^{+}$$

6) proton abstraction from multiply protontated analyte:

$$A(nH)^{n+} + M \rightarrow A((n-1)H)^{(n-1)+} + MH^{+}$$

7) matrix radical cation → protonated conversion:

$$M^{+} + M \rightarrow MH^{+} + (M-H)$$

8) protonated / sodiated matrix interconversion:

$$MNa^{+} + M \leftrightarrow MH^{+} + (M-H)Na$$

9) analyte-analyte dissimilar ion suppression:

$$A + (BNa)^{+} + M \rightarrow AH^{+} + B + (M-H)Na$$

Matrix Suppression Effect (protonating analyte):

10)

$$\begin{array}{ccccc} & & M & & M \\ M^{+} & \leftrightarrow & MH^{+} & \leftrightarrow & MNa^{+} \\ & & \downarrow A & & \\ & & AH^{+} + M & & \end{array}$$

Figures

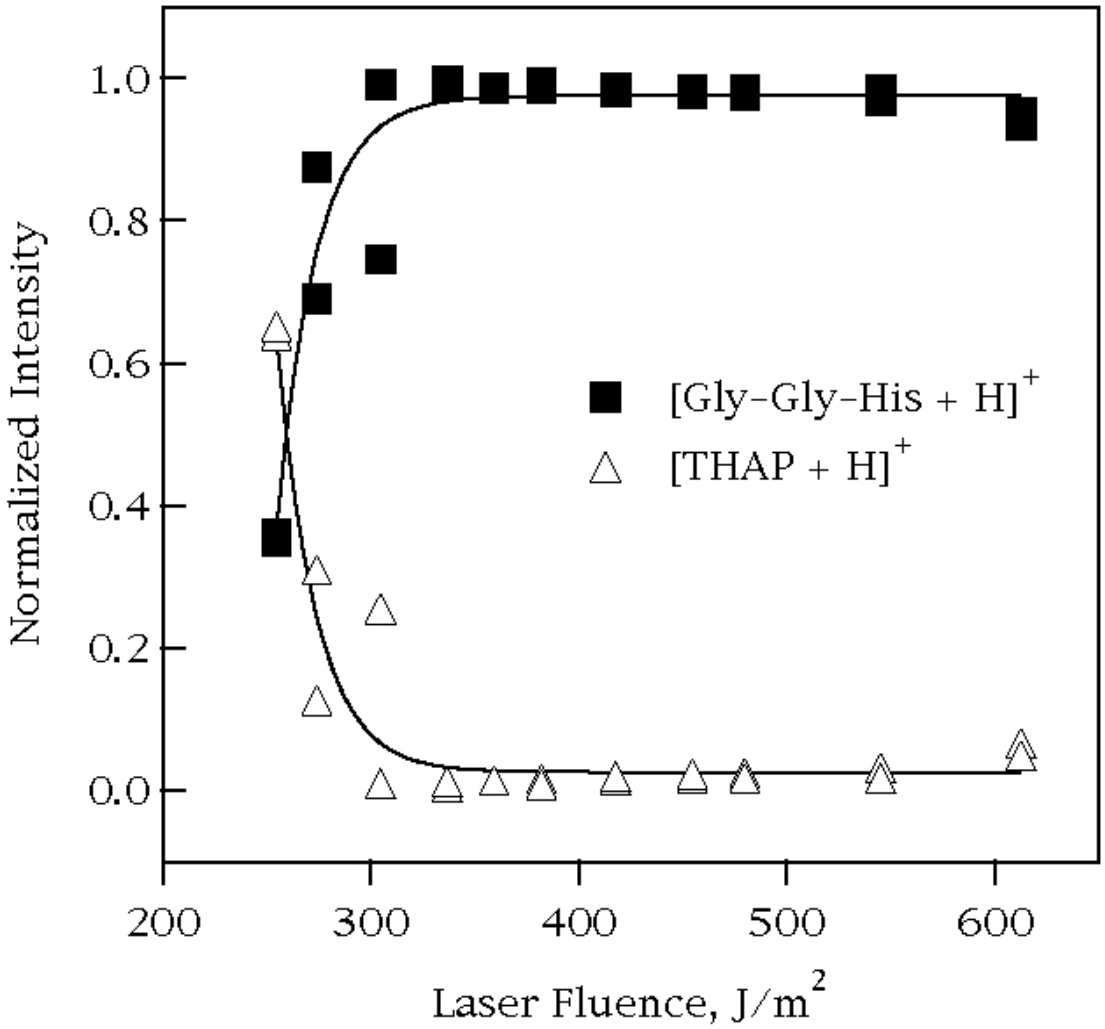

Figure 1: Normalized intensities of positive MALDI ion species obtained from a 2,4,6-trihydroxyacetophenone/glycyl-glycyl-histidine sample (1:1 molar ratio), as a function of laser fluence. The solid lines are to guide the eye.

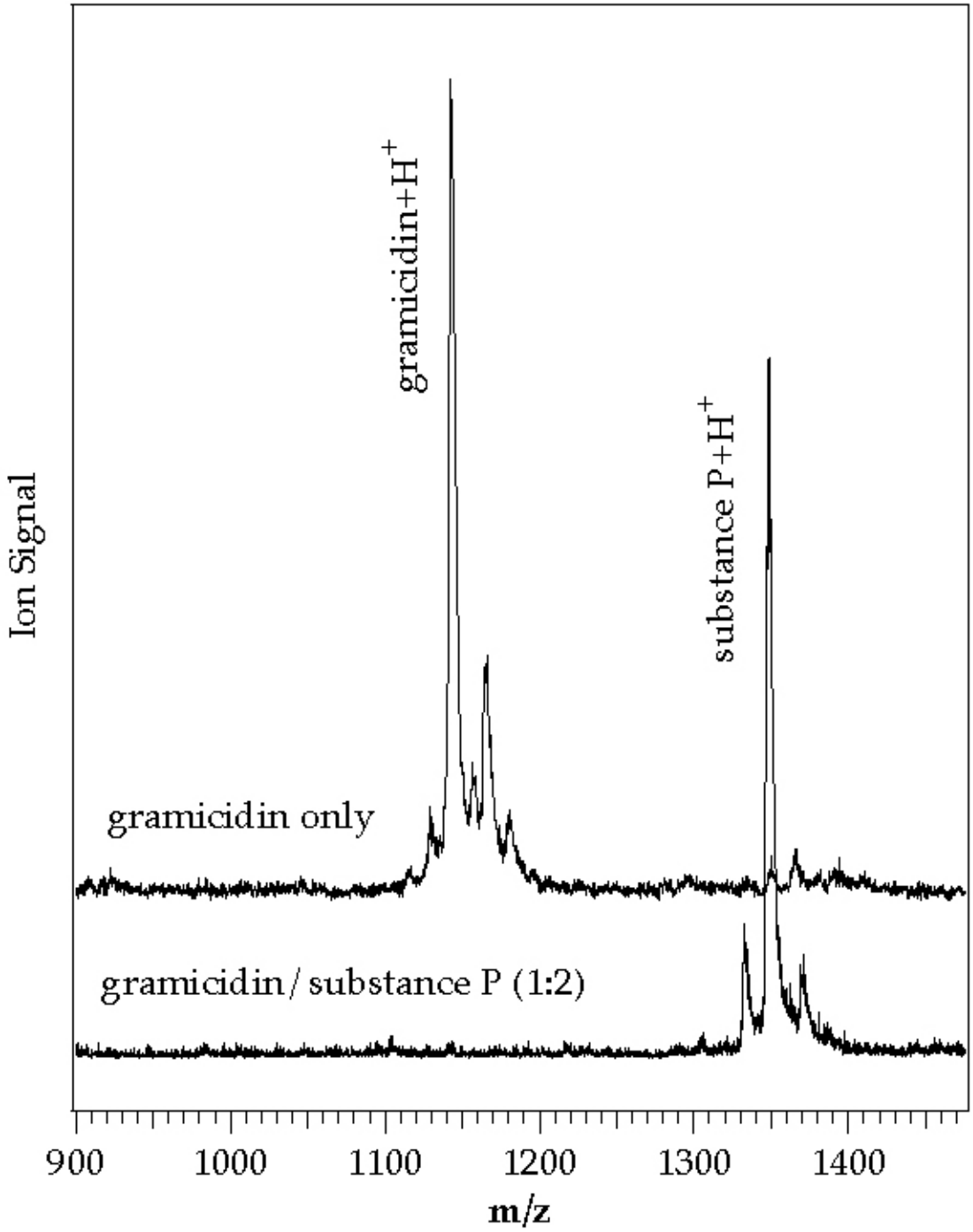

Figure 2. MALDI mass spectra of gramicidin S and of a mixture of gramicidin S and substance P in 2,5 DHB matrix (mole ratio 1:2:2000), illustrating the analyte suppression effect. The gramicidin S concentration is the same in both spectra, and the spectra were taken under identical conditions. When sufficient substance P is present the gramicidin S signal disappears.

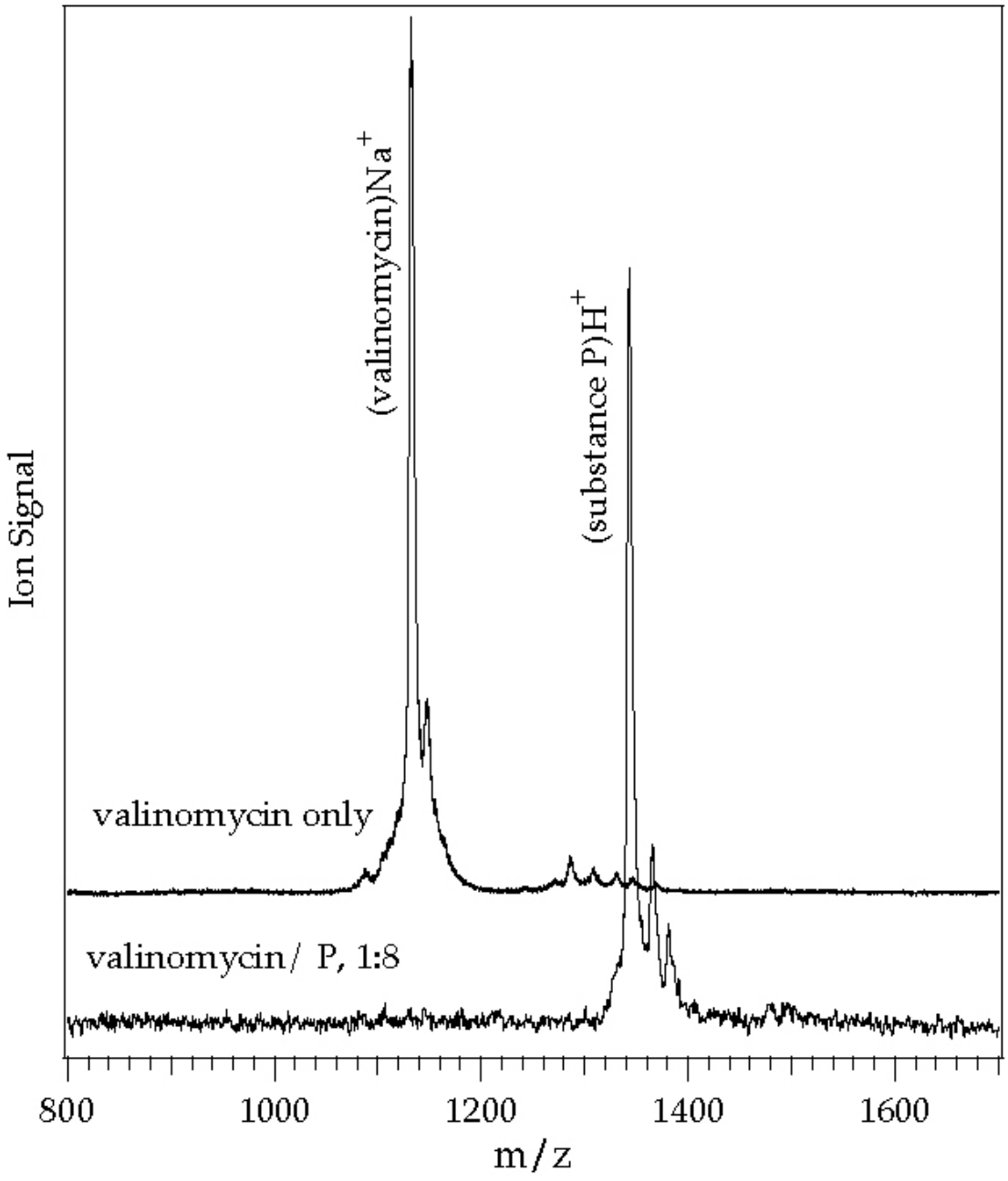

Figure 3. MALDI mass spectra of valinomycin and of a mixture of valinomycin and substance P in 2,5 DHB matrix (mole ratio 1:2.5:1000), illustrating the dissimilar analyte suppression effect. The valinomycin concentration is the same in both spectra, and the spectra were taken under identical conditions. When sufficient substance P is present the valinomycin-Na^+ signal almost completely disappears.